

Nonthermal production of WIMPs, cosmic e^\pm excesses, and γ rays from the Galactic Center

Xiao-Jun Bi,^{1,2} Robert Brandenberger,^{3,4,5,6,7} Paolo Gondolo,^{8,6} Tianjun Li,^{9,10,6} Qiang Yuan,¹ and Xinmin Zhang^{4,5,6}
¹Key Laboratory of Particle Astrophysics, Institute of High Energy Physics, Chinese Academy of Sciences, Beijing 100049, P. R. China
²Center for High Energy Physics, Peking University, Beijing 100871, P.R. China
³Department of Physics, McGill University, Montréal, QC, H3A 2T8, Canada
⁴Theoretical Physics Division, Institute of High Energy Physics, Chinese Academy of Sciences, Beijing 10049, P.R. China
⁵Theoretical Physics Center for Science Facilities (TPCSF), Chinese Academy of Sciences, P.R. China
⁶Kavli Institute for Theoretical Physics China, Chinese Academy of Sciences, Beijing 100190, P.R. China
⁷Theory Division, CERN, CH-1211 Geneva, Switzerland
⁸Department of Physics and Astronomy, University of Utah, Salt Lake City, Utah 84112, USA
⁹Key Laboratory of Frontiers in Theoretical Physics, Institute of Theoretical Physics, Chinese Academy of Sciences, Beijing 100190, P. R. China
¹⁰George P. and Cynthia W. Mitchell Institute for Fundamental Physics, Texas AM University, College Station, Texas 77843, USA
(Received 22 June 2009; published 4 November 2009)

In this paper we propose a dark matter model and study aspects of its phenomenology. Our model is based on a new dark matter sector with a $U(1)'$ gauge symmetry plus a discrete symmetry added to the standard model of particle physics. The new fields of the dark matter sector have no hadronic charges and couple only to leptons. Our model cannot only give rise to the observed neutrino mass hierarchy, but can also generate the baryon number asymmetry via nonthermal leptogenesis. The breaking of the new $U(1)'$ symmetry produces cosmic strings. The dark matter particles are produced nonthermally from cosmic string loop decay which allows one to obtain sufficiently large annihilation cross sections to explain the observed cosmic ray positron and electron fluxes recently measured by the PAMELA, ATIC, PPB-BETS, Fermi-LAT, and HESS experiments while maintaining the required overall dark matter energy density. The high velocity of the dark matter particles from cosmic string loop decay leads to a low phase space density and thus to a dark matter profile with a constant density core in contrast to what happens in a scenario with thermally produced cold dark matter where the density keeps rising towards the center. As a result, the flux of γ rays radiated from the final leptonic states of dark matter annihilation from the Galactic center is suppressed and satisfies the constraints from the HESS γ -ray observations.

DOI: [10.1103/PhysRevD.80.103502](https://doi.org/10.1103/PhysRevD.80.103502)

PACS numbers: 95.35.+d, 98.62.Gq, 98.70.Rz

I. INTRODUCTION

There is strong evidence for the existence of a substantial amount of cold dark matter (CDM). The leading CDM candidates are weakly interacting massive particles (WIMPs), for example, the lightest neutralino in supersymmetric models with R parity. With a small cosmological constant, the CDM scenario is consistent with both the observations of the large scale structure of the Universe (scales much larger than 1 Mpc) and the fluctuations of the cosmic microwave background [1].

However, the collisionless CDM scenario predicts too much power on small scales, such as a large excess of dwarf galaxies [2,3], the over-concentration of dark matter (DM) in dwarf galaxies [4–6] and in large galaxies [7]. To solve this problem, two of us with their collaborators proposed a scenario based on nonthermal production of WIMPs, which can be relativistic when generated. The WIMPs' comoving free-streaming scales could be as large as or possibly even larger than 0.1 Mpc. Then, the density fluctuations on scales less than the free-streaming scale would be suppressed [8]. Thus, the discrepancies between the observations of DM halos on subgalactic scales and the

predictions of the standard WIMP DM picture could be resolved.

Recently, the ATIC [9] and PPB-BETS [10] collaborations have reported measurements of the cosmic ray electron/positron spectrum at energies of up to ~ 1 TeV. The data shows an obvious excess over the expected background for energies in the ranges ~ 300 – 800 GeV and ~ 500 – 800 GeV, respectively. At the same time, the PAMELA collaboration also released their first cosmic-ray measurements of the positron fraction [11] and the \bar{p}/p ratio [12]. The positron fraction (but not the antiproton to proton ratio) shows a significant excess for energies above 10 GeV up to ~ 100 GeV, compared to the background predicted by conventional cosmic-ray propagation models. This result is consistent with previous measurements by HEAT [13] and AMS [14].

Very recently, the Fermi-LAT collaboration has released data on the measurement of the electron spectrum from 20 GeV to 1 TeV [15], and the HESS collaboration has published electron spectrum data from 340 GeV to 700 GeV [16], complementing their earlier measurements at 700 GeV to 5 TeV [17]. The Fermi-LAT measured spectrum agrees with ATIC below 300 GeV; however, it

does not exhibit the special features at large energy. There have already been some discussions on the implications for DM physics obtained by combining the Fermi-LAT, HESS, and PAMELA results [18].

The ATIC, PPB-BETS, and PAMELA results indicate the existence of a new source of primary electrons and positrons, while the hadronic processes are suppressed. It is well known that DM annihilation can be a possible origin for primary cosmic rays [19] which could account for the ATIC, PPB-BETS, and PAMELA data simultaneously, as discussed first in [20] and also in [21] (see [22] for a list of references).¹ However, the fact that the \bar{p}/p ratio does not show an excess gives strong constraints on DM models if they are to explain the data. In particular, it is very difficult to use well-known DM candidates like the neutralino to explain the ATIC and PAMELA data simultaneously [24] since they would also yield an excess of antiprotons. Therefore, if the observed electron/positron or positron excesses indeed arise from DM annihilation, it seems to us that there may exist special connections between the DM sector and lepton physics [25] (see also [26,27]).

In this paper, we propose a DM model and study its implications for DM detection. We fit our model to two different combinations of the experiment data: one set of data from the ATIC, PPB-BETS, and PAMELA experiments; the other from the Fermi-LAT, HESS, and PAMELA experiments. Our results show that our model can naturally explain the e^\pm excesses while at the same time solving the small-scale problems of the standard Λ CDM model via nonthermal DM production. For a single Majorana DM particle, its annihilation cross section has s wave suppression. Thus, we consider two degenerate Majorana DM particles. We add a new DM sector with a $U(1)'$ gauge symmetry and introduce an additional discrete symmetry to the standard model (SM). The DM particles are stable due to the discrete symmetry. During the $U(1)'$ gauge symmetry breaking phase transition a network of cosmic strings is generated. The decay of cosmic string loops is a channel for producing a nonthermal distribution of DM. This nonthermal distribution allows for DM masses and annihilation cross sections large enough to explain the cosmic ray anomalies while simultaneously remaining consistent with the observed DM energy density. In addition, the observed neutrino masses and mixing can be explained via the seesaw mechanism, and the baryon number asymmetry can be generated via nonthermal leptogenesis [28].

It has been recently recognized that a large annihilation cross section of DM particles into leptons to account for the cosmic ray anomalies will induce a large flux of γ rays from the Galactic Center (GC) [29] or from the centers of dwarf galaxies [30]. The predicted γ ray fluxes based on

the NFW profile for the standard CDM scenario have been shown to be in slight conflict with the current observations of HESS [31]. However, in our model the DM particles are produced nonthermally, so the high velocity of the DM particles will lower the phase space density of DM and lead to a DM profile with a constant density core [32]. Therefore, our model with nonthermally produced DM on one hand gives rise to a large annihilation cross section to account for the positron/electron excess observed locally while on the other hand it suppresses the DM density at the GC and leads to a low flux of γ ray radiation.

Our paper is organized as follows: in Sec. II, we describe in detail the model and the production mechanism of the DM particles. In Sec. III we study aspects of the phenomenology of the model, including studies of some constraints on the model parameters from particle physics experiments, implications for the PAMELA, ATIC, PPB-BETS, Fermi-LAT, and HESS results, and also the γ -ray radiation from the GC. Section IV contains the discussion and conclusions.

II. THE DARK MATTER MODEL

A. The dark matter sector

The DM model we propose consists of adding a new ‘‘DM sector’’ to the standard model. The new particles have only leptonic charges and are uncharged under color. This ensures that the DM particles annihilate preferentially into leptons. To ensure the existence of a stable DM particle, the new sector is endowed with a discrete symmetry which plays a role similar to that of R -parity in supersymmetric models. The lightest particles which are odd under the Z_2 symmetry which we introduce are the candidate DM particles.

In our convention, we denote the right-handed leptons and Higgs doublet as $e_R^i(\mathbf{1}, -1)$ and $H(\mathbf{2}, -\frac{1}{2}) = (H^0, H^-)^T$, respectively, where their $SU(2)_L \times U(1)_Y$ quantum numbers are given in parenthesis.

We consider the generalized standard model with an additional $U(1)'$ gauge symmetry broken at an intermediate scale. In particular, all the SM fermions and Higgs fields are uncharged under this $U(1)'$ gauge symmetry. To break the $U(1)'$ gauge symmetry, we introduce a SM singlet Higgs field S with $U(1)'$ charge -2 . Moreover, we introduce four SM singlet chiral fermions $\chi_1, \chi_2, N_1,$ and N_2 , a SM singlet scalar field \tilde{E} and a SM doublet scalar field H' with $SU(2)_L \times U(1)_Y$ quantum numbers $(\mathbf{1}, -1)$ and $(\mathbf{2}, \frac{1}{2})$, respectively. The $U(1)'$ charges for χ_i and H' are $\mathbf{1}$, while the $U(1)'$ charges for N_i and \tilde{E} are -1 . Thus, our model is anomaly free. To have stable DM candidates, we introduce a Z_2 symmetry. Under this Z_2 symmetry, only the particles χ_i and \tilde{E} are odd while all the other particles are even. The χ particles will be the DM candidates, whereas the chiral fermions N_i will play the role of right-handed neutrinos.

¹Note, however, that there are also astrophysical (see e.g. [23]) or other particle physics (see e.g. [22]) explanations.

The relevant part of the most general renormalizable Lagrangian consistent with the new symmetries is

$$\begin{aligned}
-\mathcal{L} = & \frac{1}{2}m_S^2 S^\dagger S + \frac{1}{2}m_{\tilde{E}}^2 \tilde{E}^\dagger \tilde{E} + \frac{1}{2}m_{H'}^2 H'^\dagger H' + \frac{\lambda}{4}(S^\dagger S)^2 + \frac{\lambda_1}{4}(\tilde{E}^\dagger \tilde{E})^2 + \frac{\lambda_2}{4}(H'^\dagger H')^2 + \frac{\lambda_3}{2}(S^\dagger S)(\tilde{E}^\dagger \tilde{E}) \\
& + \frac{\lambda_4}{2}(\tilde{E}^\dagger \tilde{E})(H'^\dagger H') + \frac{\lambda_5}{2}(S^\dagger S)(H'^\dagger H') + \frac{\lambda_6}{2}(S^\dagger S)(H^\dagger H) + \frac{\lambda_7}{2}(\tilde{E}^\dagger \tilde{E})(H^\dagger H) + \frac{\lambda_8}{2}(H'^\dagger H')(H^\dagger H) \\
& + (y_e^i \bar{e}_R^i \tilde{E} \chi_1 + y_e^i \bar{e}_R^i \tilde{E} \chi_2 + y_\chi^{ij} S \bar{\chi}_i^c \chi_j + y_N^{ij} S^\dagger N_i N_j + y_\nu^{ij} L_i H' N_j + \text{H.c.}).
\end{aligned} \tag{1}$$

As we will discuss in the following subsection, the vacuum expectation value (VEV) for S is around 10^9 GeV. Then, the couplings λ_3 , λ_5 , and λ_6 should be very small—about 10^{-12} —in order for the model to be consistent with the expected value of the SM Higgs. This fine-tuning problem could be solved naturally if we were to consider a supersymmetric model. Moreover, in order to explain the recent cosmic ray data, the Yukawa couplings y_χ^{ij} should be around 10^{-6} . This would generate a DM mass around 1 TeV. Such small Yukawa couplings y_χ^{ij} can be explained via the Froggatt-Nielsen mechanism [33] which will not be studied here.

To explain the neutrino masses and mixing via the “see-saw mechanism”, we require that the VEV of H' be about 0.1 GeV if $y_N^{ij} \sim 1$ and $y_\nu^{ij} \sim 1$. In this case, the lightest active neutrino is massless since we only have two right-handed neutrinos N_i . In addition, in our $U(1)'$ model, the Higgs field forming the strings is also the Higgs field which gives masses to the right-handed neutrinos. There are right-handed neutrinos trapped as transverse zero modes in the core of the strings. When cosmic string loops decay, they release these neutrinos. This is an out-of-equilibrium process. The released neutrinos acquire heavy Majorana masses and decay into massless leptons and electroweak Higgs particles to produce a lepton asymmetry, which is converted into a baryon number asymmetry via sphaleron transitions [28]. Thus, we can explain the baryon number asymmetry via nonthermal leptogenesis.

In this paper, we consider two degenerate Majorana DM candidates χ_1 and χ_2 since the annihilation cross section for a single Majorana DM particle is too small to explain the recent cosmic ray experiments [25]. For simplicity, we assume that the Lagrangian is invariant under $\chi_1 \leftrightarrow \chi_2$. Thus, we have

$$y_e^i \equiv y_e^i, \quad y_\chi^{ij} \equiv y_\chi^{ij}. \tag{2}$$

To make sure that we have two degenerate Majorana DM candidates χ_1 and χ_2 , we choose $y_\chi^{12} = 0$, and assume $m_\chi < m_{\tilde{E}}$.

B. Nonthermal dark matter production via cosmic strings

We assume that the $U(1)'$ gauge symmetry is broken by the VEV of the scalar field S . To be specific, we take the potential of S to be

$$V(S) = \frac{1}{4}\lambda(|S|^2 - \eta^2)^2, \tag{3}$$

where λ is the self-interaction coupling constant. The VEV of S hence is $\langle S \rangle = \eta$ with $m_S^2 = \lambda\eta^2$. Because of finite temperature effects, the symmetry is unbroken at high temperatures. During the cooling of the very early universe, a symmetry breaking phase transition takes place at a temperature T_c with

$$T_c \simeq \sqrt{\lambda}\eta. \tag{4}$$

During this phase transition, inevitably a network of local cosmic strings will be formed. These strings are topologically nontrivial field configurations formed by the Higgs field S and the $U(1)'$ gauge field A . The mass per unit length of the strings is given by $\mu = \eta^2$.

During the phase transition, a network of strings forms, consisting of both infinite strings and cosmic string loops. After the transition, the infinite string network coarsens and more loops form from the intercommuting of infinite strings. Cosmic string loops lose their energy by emitting gravitational radiation. When the radius of a loop becomes of the order of the string width $w \simeq \lambda^{-1/2}\eta^{-1}$, the loop releases its final energy into a burst of A and S particles.² Those particles subsequently decay into DM particles, with branching ratios ϵ and ϵ' . For simplicity we assume that all the final string energy goes into A particles. A single decaying cosmic string loop thus releases

$$N \simeq 2\pi\lambda^{-1}\epsilon \tag{5}$$

DM particles which we take to have a monochromatic distribution with energy $E \sim \frac{T_c}{2}$, the energy of an S -quantum in the broken phase. In our model, we assume that the masses for A , S , and N_i are roughly the same, so we have $\epsilon = 1$.

Given the symmetry we have imposed, the number densities of χ_1 and χ_2 are equal. Thus, the number density n_{DM} of DM particles, the sum of the number densities of χ_1 and χ_2 , is

$$n_{\text{DM}} \equiv n_{\chi_1} + n_{\chi_2} = 2n_{\chi_1} = 2n_{\chi_2}. \tag{6}$$

²We are not considering here DM production from cosmic string cusp annihilation since the efficiency of this mechanism may be much smaller than the upper estimate established in [34], as discussed e.g. in [35]. DM production from cusp annihilation has been considered in [36].

If the S and A quanta were in thermal equilibrium before the phase transition, then the string network is formed with a microscopic correlation length $\xi(t_c)$ (where t_c is the time at which the phase transition takes place). The correlation length gives the mean curvature radius and mean separation of the strings. As discussed in [37] (see also the reviews [38]), the initial correlation length is

$$\xi(t_c) \sim \lambda^{-1} \eta^{-1}. \quad (7)$$

After string formation, there is a time interval during which the dynamics of the strings is friction-dominated. In this period, the correlation length increases faster than the Hubble radius because loop intercommutation is very efficient. As was discussed e.g. in [39], the correlation length scale $\xi(t)$ in the friction epoch scales as

$$\xi(t) = \xi(t_c) \left(\frac{t}{t_c} \right)^{3/2}. \quad (8)$$

The friction epoch continues until $\xi(t)$ becomes comparable to the Hubble radius t . After this point, the string network follows a ‘‘scaling solution’’ with $\xi(t) \sim t$. This scaling solution continues to the present time.

The loss of energy from the network of long strings with correlation length $\xi(t)$ is predominantly due to the production of cosmic string loops. The number density of cosmic string loops created per unit of time is given by [38,39]:

$$\frac{dn}{dt} = \nu \xi^{-4} \frac{d\xi}{dt}, \quad (9)$$

where ν is a constant of order 1. We are interested in loops decaying below the temperature T_χ when the DM particles fall out of thermal equilibrium (loops decaying earlier will produce DM particles which simply thermalize). We denote the corresponding time by t_χ .

The DM number density released from t_χ till today is obtained by [8] summing up the contributions of all decaying loops. Each loop yields a number N of DM particles. We track the loops decaying at some time t in terms of the time t_f when that loop was created. Since the loop density decreases sharply as a function of time, it is the loops which decay right after t_χ which dominate the integral. For the values of $G\mu$ which we are interested in, it turns out that loops decaying around t_χ were created in the friction epoch, and the loop number density is determined by inserting (8) into (9). Changing the integration variable from t to $\xi(t)$, we integrate the redshifted number density to obtain:

$$n_{\text{DM}}^{\text{nonth}}(t_0) = N\nu \int_{\xi_F}^{\xi_0} \left(\frac{t}{t_0} \right)^{3/2} \xi^{-4} d\xi, \quad (10)$$

where the subscript 0 refers to parameters which are evaluated today. In the above, $\xi_F = \xi(t_F)$ where t_F is the time at which cosmic string loops which are decaying at the time t_χ formed.

Now the loop’s time-averaged radius (radius averaged over a period of oscillation) shrinks at a rate [38]

$$\frac{dR}{dt} = -\Gamma_{\text{loops}} G\mu, \quad (11)$$

where Γ_{loops} is a numerical factor ~ 10 – 20 . Since loops form at time t_F with an average radius

$$R(t_F) \simeq \lambda^{1/2} g_*^{3/4} G\mu M_{\text{pl}}^{1/2} t_F^{3/2}, \quad (12)$$

where g_* counts the number of massless degrees of freedom in the corresponding phase, they have shrunk to a point at the time

$$t \simeq \lambda^{1/2} g_*^{3/4} \Gamma_{\text{loops}}^{-1} M_{\text{pl}}^{1/2} t_F^{3/2}. \quad (13)$$

Thus

$$t_F \sim \lambda^{-1/3} g_*^{-1/2} \Gamma_{\text{loops}}^{2/3} M_{\text{pl}}^{-(1/3)} t_\chi^{2/3}. \quad (14)$$

Now the entropy density is

$$s = \frac{2\pi^2}{45} g_* T^3. \quad (15)$$

The time t and temperature T are related by

$$t = 0.3 g_*^{-(1/2)} (T) \frac{M_{\text{pl}}}{T^2}, \quad (16)$$

where M_{pl} is the Planck mass. Thus using Eqs. (8) and (10), we find that the DM number density today released by decaying cosmic string loops is given by

$$Y_{\text{DM}}^{\text{nonth}} \equiv \frac{n_{\text{DM}}^{\text{nonth}}}{s} = \frac{6.75}{\pi} \epsilon \nu \lambda^{3/2} \Gamma_{\text{loops}}^{-2} g_*^{3/2} g_{*t_c}^{-5/2} g_{*t_\chi}^{-5/2} M_{\text{pl}}^2 \frac{T_\chi^4}{T_c^6}, \quad (17)$$

where the subscript on g^* refers to the time when g^* is evaluated.

The DM relic abundance is related to Y_χ by

$$\begin{aligned} \Omega_\chi h^2 &\approx m_\chi Y_\chi s(t_0) \rho_c(t_0)^{-1} h^2 \\ &\approx 2.82 \times 10^8 Y_\chi^{\text{tot}} (m_\chi / \text{GeV}), \end{aligned} \quad (18)$$

where h is the Hubble parameter in units of $100 \text{ km s}^{-1} \text{ Mpc}^{-1}$, m_χ is the DM mass, and $Y_\chi^{\text{tot}} = Y_\chi^{\text{therm}} + Y_\chi^{\text{nonth}}$.

To give some concrete numbers, we choose the parameter values $\epsilon = 1$, $\nu = 1$, $\lambda = 0.5$, $\Gamma = 10$, $M_{\text{pl}} = 1.22 \times 10^{19} \text{ GeV}$, and $\Omega_\chi h^2 = 0.11$. In our model, we have $g_{*t_c} = 136$, $g_{*t_F} = 128$, and $g_{*t_\chi} = 128$. We define the dimensionless ratios

$$\alpha \equiv \frac{m_\chi}{T_\chi}, \quad \beta \equiv \frac{Y_\chi^{\text{nonth}}}{Y_\chi^{\text{tot}}}. \quad (19)$$

Demanding that we obtain a specific value of β for the above choices of the parameter values will fix T_c via (18). For various values of α and β , we present the resulting T_c

TABLE I. The required T_c values in units of GeV for various choices of α and β in the cases $m_\chi = 620$ GeV, $m_\chi = 780$ GeV, and $m_\chi = 1500$ GeV, respectively.

α	1	1	2	2	5	5
β	1	0.5	1	0.5	1	0.5
T_c ($m_\chi = 620$ GeV)	7.7×10^9	8.6×10^9	4.8×10^9	5.4×10^9	2.6×10^9	2.9×10^9
T_c ($m_\chi = 780$ GeV)	9.3×10^9	1.0×10^{10}	5.9×10^9	6.6×10^9	3.2×10^9	3.6×10^9
T_c ($m_\chi = 1500$ GeV)	1.6×10^{10}	1.8×10^{10}	1.0×10^{10}	1.1×10^{10}	5.5×10^9	6.2×10^9
α	10	10	15	15	20	20
β	1	0.5	1	0.5	1	0.5
T_c ($m_\chi = 620$ GeV)	1.7×10^9	1.9×10^9	1.3×10^9	1.4×10^9	1.0×10^9	1.2×10^9
T_c ($m_\chi = 780$ GeV)	2.0×10^9	2.2×10^9	1.5×10^9	1.7×10^9	1.3×10^9	1.4×10^9
T_c ($m_\chi = 1500$ GeV)	3.5×10^9	3.9×10^9	2.6×10^9	3.0×10^9	2.2×10^9	2.4×10^9

values for the cases $m_\chi = 620$ GeV, $m_\chi = 780$ GeV, and $m_\chi = 1500$ GeV, respectively, in Table I. In short, T_c must be around 10^9 GeV if we want to generate enough DM density nonthermally via cosmic strings.

III. PHENOMENOLOGY OF THE MODEL

A. Constraints on the model parameters

The coupling constants y_e^i between right-handed leptons and the DM sector are constrained by experiments, and especially by the precise value of muon anomalous magnetic moment $g - 2$. Assuming that the masses of χ and \tilde{E} are nearly degenerate, we obtain that the contribution to the muon anomalous magnetic moment from the new coupling is about [40]

$$\delta a_i \sim (y_e^i)^2 \frac{1}{192\pi^2} \frac{m_{e_i}^2}{m_\chi^2}. \quad (20)$$

The 2σ upper bound from the E821 Collaboration on δa_μ is smaller than $\sim 40 \times 10^{-10}$ [41], from which we get for $m_\chi \sim 1$ TeV,

$$y_\mu \lesssim 10. \quad (21)$$

For the electron anomalous magnetic momentum we assume the contribution from the dark sector is within the experimental error [42]

$$\delta a_e \leq 7 \times 10^{-13}. \quad (22)$$

Then we get a upper limit on y_e which is about 30. Therefore the constraints on the couplings of the model due to the heavy masses of the new particles are quite loose.

Now we study the constraints from the experimental limits on lepton flavor violation (LFV) processes such as

$\mu \rightarrow e\gamma$, $\tau \rightarrow \mu(e)\gamma$ and so on. The branching ratios for the radiative LFV processes are given by [40]

$$\text{Br}(e_i \rightarrow e_j\gamma) \sim \alpha_{em} m_i^5 / 2 \times \left(\frac{Y_e^i Y_e^j}{384\pi^2 m_\chi^2} \right)^2 / \Gamma_i, \quad (23)$$

where Γ_i is the width of e_i . Given the experimental constraint on the process $\mu \rightarrow e\gamma$ we get

$$\text{Br}(\mu \rightarrow e\gamma) \sim 10^{-8} \times (y_e y_\mu)^2 \lesssim 10^{-11}, \quad (24)$$

which gives that $y_e y_\mu \lesssim 0.03$. For the process $\tau \rightarrow \mu(e)\gamma$ we have

$$\text{Br}(\tau \rightarrow \mu(e)\gamma) \sim 10^{-9} \times (y_{\mu(e)} y_\tau)^2 \lesssim 10^{-7}, \quad (25)$$

which leads to the conclusion that $y_\tau y_{\mu(e)} \lesssim 10$. Connecting the DM sector to the PAMELA and Fermi-LAT (or ATIC) results usually requires a large branching ratio into electron and positron pairs. From the LFV constraints shown above we conclude that it is possible to have a large branching ratio for the annihilation of the DM particles directly into e^+e^- , or via $\mu^+\mu^-$.

B. Explanation for the cosmic e^\pm excesses

In our model the DM sector only couples to the SM lepton sector. Therefore DM annihilates into leptons dominantly. Furthermore, since DM is produced nonthermally in our model the DM annihilation rates can be quite large with a sizable Yukawa coupling y_e^i . Thus our model can naturally explain the cosmic e^\pm excesses observed.

Because the annihilation cross sections for $\chi_1\chi_1$ and $\chi_2\chi_2$ to leptons are s wave suppressed, the dominant cross sections of $\chi_1\chi_2$ annihilating into charged leptons are given by [25]

$$\begin{aligned}
 \sigma_{ij}v &\equiv \sigma_{\chi_1\chi_2 \rightarrow e_R^i e_R^j} v \\
 &= \frac{4}{32\pi} |y_e^i|^2 |y_e^j|^2 \frac{1}{s\sqrt{s(s-4m_\chi^2)}} \left\{ \sqrt{s(s-4m_\chi^2)} + \left[2(m_E^2 - m_\chi^2) - \frac{2m_\chi^2 s}{s+2m_E^2-2m_\chi^2} \right] \right. \\
 &\quad \times \ln \left| \frac{s+2m_E^2-2m_\chi^2 - \sqrt{s(s-4m_\chi^2)}}{s+2m_E^2-2m_\chi^2 + \sqrt{s(s-4m_\chi^2)}} \right| + 2(m_E^2 - m_\chi^2)^2 \left[\frac{1}{s+2m_E^2-2m_\chi^2 - \sqrt{s(s-4m_\chi^2)}} \right. \\
 &\quad \left. \left. - \frac{1}{s+2m_E^2-2m_\chi^2 + \sqrt{s(s-4m_\chi^2)}} \right] \right\}, \tag{26}
 \end{aligned}$$

where v is the relative velocity between the two annihilating particles in their center of mass system. The overall factor 4 will be canceled when we calculate the lepton fluxes, so, we will leave it in our discussions. Up to $\mathcal{O}(v^2)$, the above cross section can be simplified as [25]

$$\begin{aligned}
 \sigma_{ij}v &\simeq \frac{4}{128\pi} |y_e^i|^2 |y_e^j|^2 \left\{ \frac{8}{(2+r)^2} \right. \\
 &\quad \left. + \left[\frac{1}{(2+r)^2} - \frac{8}{(2+r)^3} \right] v^2 \right\} \frac{1}{m_\chi^2}, \tag{27}
 \end{aligned}$$

where

$$r \equiv \frac{m_E^2 - m_\chi^2}{m_\chi^2} > 0. \tag{28}$$

With $v \sim 10^{-3}$ and $r \sim 0$, we obtain [25]

$$\langle \sigma_{ij}v \rangle \simeq 4 \times 1.2 \times 10^{-25} \text{ cm}^3 \text{ sec}^{-1} \left(\frac{700 \text{ GeV}}{m_\chi} \right)^2 |y_e^i|^2 |y_e^j|^2. \tag{29}$$

We emphasize that the Yukawa couplings y_e^i should be smaller than $\sqrt{4\pi}$ for the perturbative analysis to be valid.

In our model with nonthermal production of DM particles, we consider two separate fits to the ATIC/PPB-BETS/PAMELA and Fermi-LAT/HESS/PAMELA data sets. Firstly we consider a numerical fit to the ATIC, PPB-BETS and PAMELA data [25]. In this case we assume the DM mass to be 620 GeV and that DM annihilates into electron/positron pairs predominantly, i.e., $y_e^i \sim 0$ for $i = 2, 3$. In the second case we fit the Fermi-LAT, HESS and PAMELA data by taking the DM mass 1500 GeV and assuming that DM annihilates into $\mu^+\mu^-$ pairs dominantly. Note that all lepton fluxes resulting from DM annihilation are proportional to $n_\chi^2 \sigma_{\text{ann}}$ for models with a single DM candidate χ . Because $n_{\chi_1} = n_{\chi_2} = n_\chi/2$ in our

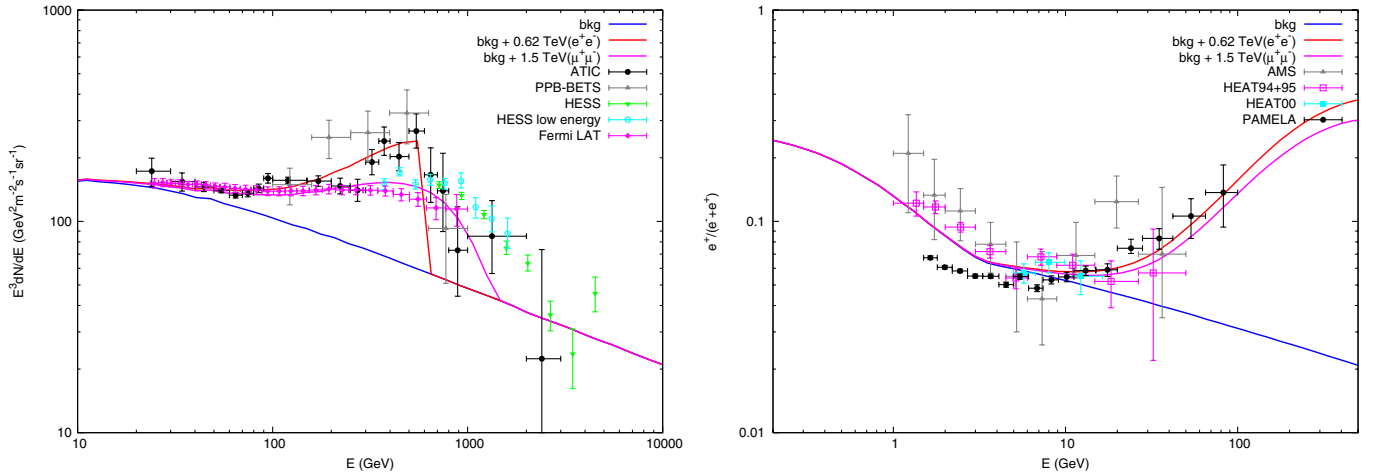


FIG. 1 (color online). Left: The $e^+ + e^-$ spectrum including the contribution from DM annihilation compared with the observational data from ATIC [9], PPB-BETS [10], HESS [16,17], and Fermi-LAT [15]. Right: The $e^+/(e^+ + e^-)$ ratio including the contribution from DM annihilation as a function of energy compared with the data from AMS [14], HEAT [13,49], and PAMELA [11]. Two sets of fitting parameters are considered: in one model (Model I) the DM mass is 620 GeV with e^+e^- being the main annihilation channel to fit the ATIC data, while in the other model (Model II) the DM mass is 1500 GeV and we assume that $\mu^+\mu^-$ is the main annihilation channel to fit the Fermi-LAT data.

TABLE II. Parameters of the two scenarios adopted to fit the ATIC/PPB-BETS/PAMELA or Fermi-LAT/HESS/PAMELA data.

	channel	m_χ (GeV)	$\langle\sigma v\rangle$ (10^{-23} cm 3 s $^{-1}$)	$J_{\Delta\Omega}^{\max}$	$J_{\Delta\Omega}^{1\sigma}$	$J_{\Delta\Omega}^{2\sigma}$
Model I	e^+e^-	620	0.75	300	42	97
Model II	$\mu^+\mu^-$	1500	3.6	200	81	111

model, the lepton fluxes are proportional to

$$n_{\chi_1} n_{\chi_2} \sigma_{\text{ann}} = \frac{1}{4} n_\chi^2 \sigma_{\text{ann}}. \quad (30)$$

This will cancel the overall factor 4 in the above annihilation cross sections in Eqs. (26) and (27).

In Fig. 1 we show that both cases can give a good fit to the data after considering the propagation of electrons and positrons in interstellar space [25] with the annihilation cross section 0.75×10^{-23} cm 3 s $^{-1}$ and 3.6×10^{-23} cm 3 s $^{-1}$, respectively. The model parameters of the two fits are given in Table II. For the first fit, we do not need the boost factor at all by choosing $y_e^1 = 2.6$, which is still smaller than the upper limit $\sqrt{4\pi}$ for a valid perturbative theory. Moreover, choosing $y_e^2 = 3$ in the second fit, we just need a small boost factor at the order of 10 which may be due to the clumps of the DM distribution [43] or uncertainties of the propagation model and local dark matter density.³ Therefore, the results on the observed cosmic e^\pm excesses are possibly explained in our model.

C. γ -ray radiation from the galactic center

Since the explanations of the anomalous cosmic ray require a very large annihilation cross section to account for the observational results, this condition leads to a strong γ -ray radiation from the final lepton states. In particular, observations of the GC [29] or the center of dwarf galaxies [30] have already led to constraints on the flux of the γ -ray radiation.

The HESS observation of γ -rays from the GC [31] sets constraints on the Galactic DM profile. The NFW profile in the standard CDM scenario leads to too large a flux of γ -rays, thus conflicting with the HESS observation. On the other hand, if DM is produced nonthermally as suggested in Sec. II the DM profile will have a constant density core

³It should be noted that enhancement due to DM clumps is at most a few and will be hard to reach ~ 10 [43] especially in our model that the phase density is enlarged by nonthermal production. See more discussions in the next subsection. However, considering that the boost factor is given in a specific propagation model and the local DM density is set as 0.3 GeV cm $^{-3}$ we think it is not necessary to be too serious about this factor. For example the local density can be 2 times larger than 0.3 GeV cm $^{-3}$ either due to the uncertainty of measurement or probably because we lie in a DM clump. The boost factor can also be large if we happen to be close to a nearby DM clump.

[32] so that the γ -ray radiation from the GC will be greatly suppressed.

In our numerical studies, we consider the following two cases to constrain the DM profile:

- (i) Case I: we simply require that the γ -ray flux due to final state radiation (FSR) do not exceed the HESS observation.
- (ii) Case II: we make a global fit to the HESS data by assuming an astrophysical source with power law spectrum plus an additional component from FSR resulting from DM annihilation.

Let us consider a DM profile taking the form

$$\rho(r) = \frac{\rho_s}{\left(\frac{r}{r_s}\right)^\gamma (1 + \frac{r}{r_s})^{3-\gamma}}, \quad (31)$$

where ρ_s is the scale density and $r_s \equiv r_{\text{vir}}/c_{\text{vir}}(2 - \gamma)$ is the scale radius, with r_{vir} the virial radius of the halo⁴ and c_{vir} the concentration parameter. In this work the concentration parameter c_{vir} and shape parameter γ are left free, and we normalize the local DM density to be 0.3 GeV cm $^{-3}$. Then the virial radius and total halo mass are solved to get self-consistent values. Given the density profile, the γ -ray flux along a specific direction can be written as

$$\begin{aligned} \phi(E, \psi) &= C \times W(E) \times J(\psi) \\ &= \frac{\rho_\odot^2 R_\odot}{4\pi} \times \frac{\langle\sigma v\rangle}{2m_\chi^2} \frac{dN}{dE} \times \frac{1}{\rho_\odot^2 R_\odot} \int_{\text{LOS}} \rho^2(l) dl, \end{aligned} \quad (32)$$

where the integral is taken along the line-of-sight, $W(E)$ and $J(\psi)$ represent the particle physics factor and the astrophysical factor, respectively. Thus, if the particle physics factor is fixed using the locally observed e^+e^- fluxes, we can get constraints on the astrophysical factor, and hence the DM density profile, according to the γ -ray flux. For the emission from a diffuse region with solid angle $\Delta\Omega$, we define the average astrophysical factor as

$$J_{\Delta\Omega} = \frac{1}{\Delta\Omega} \int_{\Delta\Omega} J(\psi) d\Omega. \quad (33)$$

It should be noted that the HESS observation on the GC γ -ray flux is a background subtracted one [31]. In [31] the emission from $0.8^\circ < |b| < 1.5^\circ$, $|l| < 0.8^\circ$ is taken as the background. Therefore the HESS reported result is not the total emission of the selected sky region, but a lowered one after subtracting the background. To compare the γ -ray flux emitted by DM annihilation at the GC region we follow the method adopted in [45], i.e., we calculate the γ -ray flux from DM in the HESS signal region ($|b| < 0.3^\circ$,

⁴The virial radius is usually defined as the range inside which the average density of DM is some factor of the critical density ρ_c , e.g., $18\pi^2 + 82x - 39x^2$ with $x = \Omega_M(z) - 1 = -\frac{\Omega_\Lambda}{\Omega_M(1+z)^3 + \Omega_\Lambda}$ for a Λ CDM universe [44].

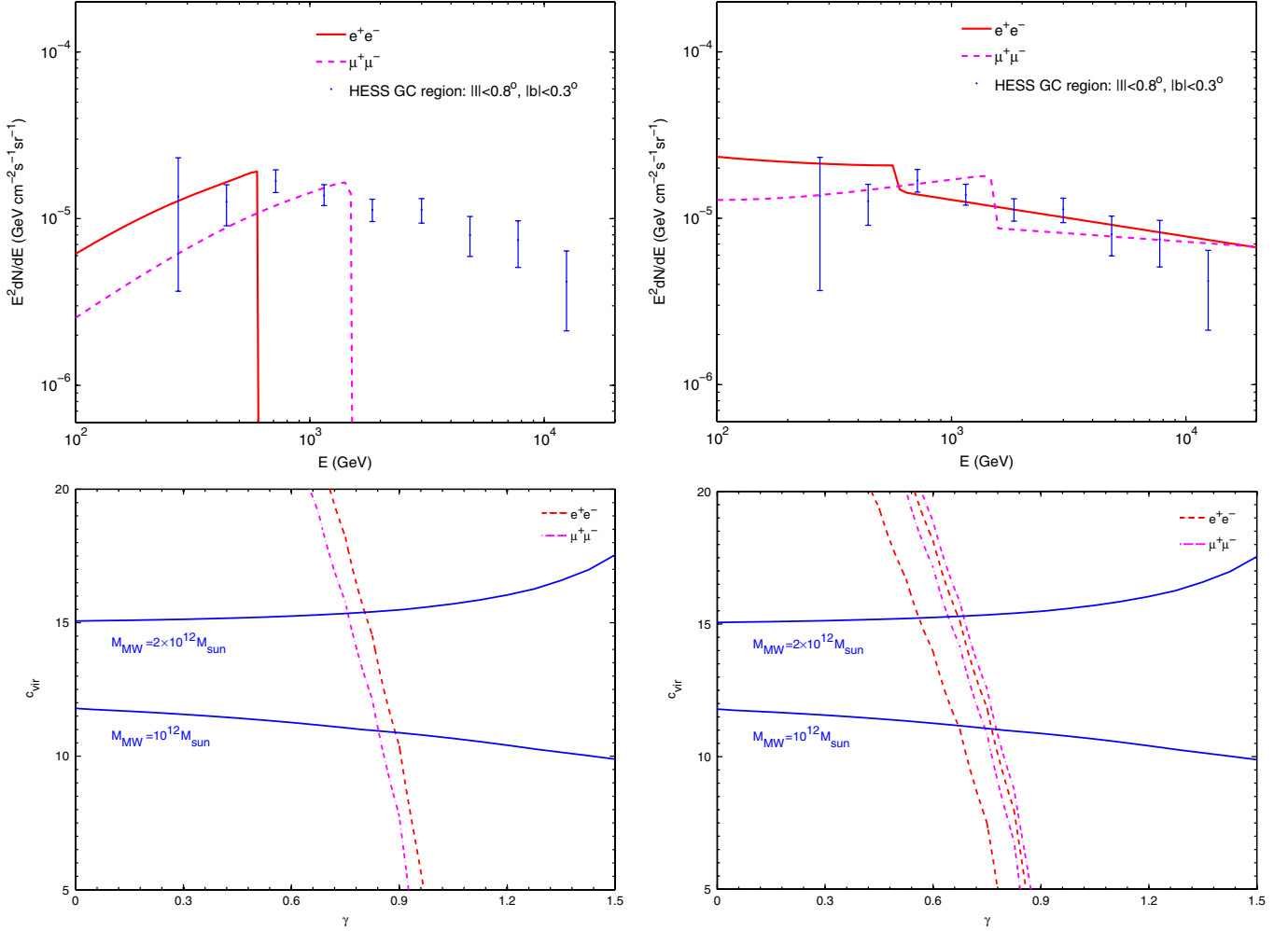


FIG. 2 (color online). Upper: the FSR γ -ray fluxes from a region with $|l| < 0.8^\circ$ and $|b| < 0.3^\circ$ close to GC compared with the observational data from HESS [31]. The left panel compares the two models given in Table II directly with the data, while the right panel shows the combined fitting results using a power law astrophysical background together with the FSR contribution from DM annihilation at 95% (2σ) confidence level. Lower: constraints on the DM profile parameters γ and c_{vir} due to the HESS observation of γ -ray radiation from the GC by assuming different final leptonic states. The left panel corresponds to the constraint Case I, while the right panel corresponds to Case II. The two curves in the right panel represent the 1σ and 2σ upper bounds, respectively.

$|l| < 0.8^\circ$) with subtracting the one in the HESS background region ($0.8^\circ < |b| < 1.5^\circ$, $|l| < 0.8^\circ$), and then compare the calculation with the data. Thus the $J_{\Delta\Omega}$ factor actually means $J_{\Delta\Omega}^{\text{sig}} - J_{\Delta\Omega}^{\text{bkg}}$ in the following.

The constraints on the average astrophysical factor $J_{\Delta\Omega}$ for the two models are gathered in Table II, in which $J_{\Delta\Omega}^{\text{max}}$ shows the maximum J factor corresponding to Case I, while $J_{\Delta\Omega}^{1\sigma, 2\sigma}$ corresponds to Case II, at the 68% (1σ) and 95% (2σ) confidence levels. The γ -ray fluxes of the two cases are shown in the upper panels of Fig. 2.

In the lower panels of Fig. 2 we show the iso- $J_{\Delta\Omega}$ lines in the $\gamma - c_{\text{vir}}$ plane for Case I (left) and Case II (right), respectively. In this figure we also show the mass condition of $(1 - 2) \times 10^{12} M_\odot$ of the Milky Way halo. From Fig. 2 we can see that the NFW profile with $\gamma = 1$ (chosen based on N-body simulation in the standard CDM scenario) is

constrained by the HESS data, if the observed cosmic e^\pm excesses are interpreted as DM annihilation. However, if DM is produced nonthermally the high velocity of the DM particle will make the DM behave like warm DM and lead to a flat DM profile which suppresses the γ -ray flux from the GC.

IV. DISCUSSION AND CONCLUSIONS

In this paper we have proposed a DM model and studied aspects of its phenomenology. We have shown that our model can simultaneously explain the cosmic ray anomalies recently measured by the ATIC, PPB-BETS, and PAMELA experiments or by the Fermi-LAT, HESS, and PAMELA experiments, resolve the small-scale structure problems of the standard Λ CDM paradigm, explain the observed neutrino mass hierarchies, explain the baryon

number asymmetry via nonthermal leptogenesis and suppress the γ ray radiation from the GC.

In this model, DM couples only to leptons. In direct detection experiments it would show as an “electromagnetic” event rather than a nuclear recoil. Experiments that reject electromagnetic events would thus be ignoring the signal. However, in the Fermi-LAT/HESS/PAMELA fits, the DM particle couples mainly to muons, and there being no muons in the target of direct detection experiments, no significant signal would be expected. In the ATIC/PPB-BETS/PAMELA fit, the DM couples predominantly to electrons; the electron recoil energy is of order $m_e v_{\text{DM}}^2 \sim 0.1$ eV, and it would be too small to be detectable in current devices. Alternatively, this energy could cause fluorescence [46], albeit the fluorescence cross section would be prohibitively small. Regarding the annual modulation signal observed by DAMA [47], although this experiment accepts all recoil signals, an estimate of the electron scattering cross section shows that the present model predicts a cross section which is about 8 orders of magnitude smaller than ~ 1 pb required to account for the modulation [26]. Therefore we do not expect a signal in direct detection experiments if the DM model presented here is realized. In addition, the capture of DM particles in the Sun or the Earth is also impossible since the DM will not lose its kinetic energy when scattering with electrons in the Sun. Therefore we do not expect high energy neutrino signals from the Sun or the Earth either.

Finally, we should point out that there are constraints on the DM annihilation cross sections from cosmic micro-

wave background (CMB) observations by e.g. Wilkinson Microwave Anisotropy Probe (WMAP) [48]. It is an independent way to probe the DM properties besides the cosmic ray observations. Our results in this work are consistent with the 95% limit from WMAP. The future Planck data will either confirm or exclude the DM annihilation scenario to explain the cosmic e^\pm excesses, as the model suggested in this work.

ACKNOWLEDGMENTS

We thank Pei-Hong Gu for helpful discussions. We wish to acknowledge the hospitality of the KITPC under their program “Connecting Fundamental Theory with Cosmological Observations” during which the ideas reported here were discussed. This work was supported in part by the Natural Sciences Foundation of China (Nos. 10773011, 10821504, 10533010, 10675136), by the Chinese Academy of Sciences under the Grant No. KJCX3-SYW-N2, by the Cambridge-Mitchell Collaboration in Theoretical Cosmology, and by the Project of Knowledge Innovation Program (PKIP) of Chinese Academy of Sciences, Grant No. KJCX2.YW.W10. R. B. wishes to thank the Theory Division of the Institute of High Energy Physics (IHEP) and the CERN Theory Division for hospitality and financial support. R. B. is also supported by an NSERC Discovery Grant and by the Canada Research Chairs Program. P. G. thanks IHEP for hospitality and acknowledges support from the NSF Grant No. PHY-0756962.

-
- [1] N. A. Bahcall, J. P. Ostriker, S. Perlmutter, and P. J. Steinhardt, *Science* **284**, 1481 (1999).
 - [2] A. A. Klypin, A. V. Kravtsov, O. Valenzuela, and F. Prada, *Astrophys. J.* **522**, 82 (1999).
 - [3] B. Moore, F. Governato, T. R. Quinn, J. Stadel, and G. Lake, *Astrophys. J.* **499**, L5 (1998).
 - [4] B. Moore, *Nature (London)* **370**, 629 (1994).
 - [5] A. Burkert, *IAU Symposium / Symp-Int.Astron.Union* **171**, 175 (1996); *Astrophys. J.* **447**, L25 (1995).
 - [6] S. S. McGaugh and W. J. G. de Blok, *Astrophys. J.* **499**, 41 (1998).
 - [7] J. F. Navarro and M. Steinmetz, *Astrophys. J.* **528**, 607 (2000).
 - [8] W. B. Lin, D. H. Huang, X. Zhang, and R. H. Brandenberger, *Phys. Rev. Lett.* **86**, 954 (2001); R. Jeannerot, X. Zhang, and R. H. Brandenberger, *J. High Energy Phys.* **12** (1999) 003.
 - [9] J. Chang *et al.*, *Nature (London)* **456**, 362 (2008).
 - [10] S. Torii *et al.* (PPB-BETS Collaboration), arXiv:0809.0760.
 - [11] O. Adriani *et al.* (PAMELA Collaboration), *Nature (London)* **458**, 607 (2009).
 - [12] O. Adriani *et al.*, *Phys. Rev. Lett.* **102**, 051101 (2009).
 - [13] S. W. Barwick *et al.* (HEAT Collaboration), *Astrophys. J.* **482**, L191 (1997).
 - [14] M. Aguilar *et al.* (AMS-01 Collaboration), *Phys. Lett. B* **646**, 145 (2007).
 - [15] Fermi Collaboration, *Phys. Rev. Lett.* **102**, 181101 (2009).
 - [16] H.E.S.S. Collaboration, arXiv:0905.0105.
 - [17] F. Aharonian *et al.* (H.E.S.S. Collaboration), *Phys. Rev. Lett.* **101**, 261104 (2008).
 - [18] L. Bergstrom, J. Edsjo, and G. Zaharijas, *Phys. Rev. Lett.* **103**, 031103 (2009); S. Shirai, F. Takahashi, and T. T. Yanagida, *Phys. Lett. B* **680**, 485 (2009); D. Grasso *et al.*, *Astropart. Phys.* **32**, 140 (2009); C. H. Chen, C. Q. Geng, and D. V. Zhuridov, arXiv:0905.0652.
 - [19] S. Rudaz and F. W. Stecker, *Astrophys. J.* **325**, 16 (1988); J. R. Ellis, R. A. Flores, K. Freese, S. Ritz, D. Seckel, and J. Silk, *Phys. Lett. B* **214**, 403 (1988); M. S. Turner and F. Wilczek, *Phys. Rev. D* **42**, 1001 (1990); M. Kamionkowski and M. S. Turner, *Phys. Rev. D* **43**, 1774 (1991); A. J. Tylka, *Phys. Rev. Lett.* **63**, 840 (1989); **63**, 1658(E) (1989); A. J. Tylka and D. Eichler, E. A. Baltz, and J. Edsjo, *Phys. Rev. D* **59**, 023511 (1998); G. L. Kane,

- L. T. Wang, and J.D. Wells, Phys. Rev. D **65**, 057701 (2002); E. A. Baltz, J. Edsjo, K. Freese, and P. Gondolo, Phys. Rev. D **65**, 063511 (2002).
- [20] V. Barger, W. Y. Keung, D. Marfatia, and G. Shaughnessy, Phys. Lett. B **672**, 141 (2009); M. Cirelli, M. Kadastik, M. Raidal, and A. Strumia, Nucl. Phys. **B813**, 1 (2009); N. Arkani-Hamed, D. P. Finkbeiner, T. R. Slatyer, and N. Weiner, Phys. Rev. D **79**, 015014 (2009); M. Fairbairn and J. Zupan, J. Cosmol. Astropart. Phys. 07 (2009) 001; A. E. Nelson and C. Spitzer, arXiv:0810.5167; I. Cholis, D. P. Finkbeiner, L. Goodenough, and N. Weiner, arXiv:0810.5344; Y. Nomura and J. Thaler, Phys. Rev. D **79**, 075008 (2009); D. Feldman, Z. Liu, and P. Nath, Phys. Rev. D **79**, 063509 (2009); P. F. Yin, Q. Yuan, J. Liu, J. Zhang, X. J. Bi, S. H. Zhu, and X. M. Zhang, Phys. Rev. D **79**, 023512 (2009); K. Ishiwata, S. Matsumoto, and T. Moroi, Phys. Lett. B **675**, 446 (2009).
- [21] J. Zhang, X. J. Bi, J. Liu, S. M. Liu, P. F. Yin, Q. Yuan, and S. H. Zhu, Phys. Rev. D **80**, 023007 (2009); F. Chen, J. M. Cline, and A. R. Frey, Phys. Rev. D **79**, 063530 (2009).
- [22] R. Brandenberger, Y. F. Cai, W. Xue, and X. M. Zhang, arXiv:0901.3474.
- [23] D. Hooper, P. Blasi, and P. D. Serpico, J. Cosmol. Astropart. Phys. 01 (2009) 025; H. Yuksel, M. D. Kistler, and T. Stanev, Phys. Rev. Lett. **103**, 051101 (2009); J. Hall and D. Hooper, arXiv:0811.3362; S. Profumo, arXiv:0812.4457; H. B. Hu, Q. Yuan, B. Wang, C. Fan, J. L. Zhang, and X. J. Bi, Astrophys. J. **700**, L170 (2009); D. Malyshev, I. Cholis, and J. Gelfand, Phys. Rev. D **80**, 063005 (2009).
- [24] M. Cirelli and A. Strumia, arXiv:0808.3867; F. Donato, D. Maurin, P. Brun, T. Delahaye, and P. Salati, Phys. Rev. Lett. **102**, 071301 (2009).
- [25] X. J. Bi, P. H. Gu, T. Li, and X. Zhang, J. High Energy Phys. 04 (2009) 103.
- [26] P. J. Fox and E. Poppitz, Phys. Rev. D **79**, 083528 (2009).
- [27] R. Allahverdi, B. Dutta, K. Richardson-McDaniel, and Y. Santoso, Phys. Rev. D **79**, 075005 (2009); S. Khalil, H. S. Lee, and E. Ma, Phys. Rev. D **79**, 041701 (2009).
- [28] R. Jeannerot, Phys. Rev. Lett. **77**, 3292 (1996).
- [29] L. Bergstrom, G. Bertone, T. Bringmann, J. Edsjo, and M. Taoso, Phys. Rev. D **79**, 081303 (2009).
- [30] R. Essig, N. Sehgal, and L. E. Strigari, Phys. Rev. D **80**, 023506 (2009).
- [31] F. Aharonian *et al.* (H.E.S.S. Collaboration), Nature (London) **439**, 695 (2006).
- [32] X. J. Bi, M. Z. Li, and X. M. Zhang, Phys. Rev. D **69**, 123521 (2004); J. A. R. Cembranos, J. L. Feng, A. Rajaraman, and F. Takayama, Phys. Rev. Lett. **95**, 181301 (2005); M. Kaplinghat, Phys. Rev. D **72**, 063510 (2005).
- [33] C. D. Froggatt and H. B. Nielsen, Nucl. Phys. **B147**, 277 (1979).
- [34] R. H. Brandenberger, Nucl. Phys. **B293**, 812 (1987).
- [35] J. J. Blanco-Pillado and K. D. Olum, Phys. Rev. D **59**, 063508 (1999).
- [36] Y. Cui and D. E. Morrissey, Phys. Rev. D **79**, 083532 (2009).
- [37] T. W. B. Kibble, Phys. Rep. **67**, 183 (1980); Acta Phys. Pol. B **13**, 723 (1982).
- [38] A. Vilenkin and E. P. S. Shellard, *Cosmic Strings and Other Topological Defects* (Cambridge University Press, Cambridge, England, 1994); M. B. Hindmarsh and T. W. B. Kibble, Rep. Prog. Phys. **58**, 477 (1995); R. H. Brandenberger, Int. J. Mod. Phys. A **9**, 2117 (1994).
- [39] R. H. Brandenberger and A. Riotto, Phys. Lett. B **445**, 323 (1999).
- [40] X. J. Bi, Y. P. Kuang, and Y. H. An, Eur. Phys. J. C **30**, 409 (2003).
- [41] G. W. Bennett *et al.* (Muon $g - 2$ Collaboration), Phys. Rev. Lett. **89**, 101804 (2002); **89**, 129903 (2002).
- [42] C. Amsler *et al.* (Particle Data Group), Phys. Lett. B **667**, 1 (2008).
- [43] Q. Yuan and X. J. Bi, J. Cosmol. Astropart. Phys. 05 (2007) 001; J. Lavalle, Q. Yuan, D. Maurin, and X. J. Bi, Astron. Astrophys. **479**, 427 (2008).
- [44] G. L. Bryan and M. L. Norman, Astrophys. J. **495**, 80 (1998).
- [45] G. D. Mack, T. D. Jacques, J. F. Beacom, N. F. Bell, and H. Yuksel, Phys. Rev. D **78**, 063542 (2008).
- [46] G. D. Starkman and D. N. Spergel, Phys. Rev. Lett. **74**, 2623 (1995).
- [47] R. Bernabei *et al.*, Phys. Rev. D **77**, 023506 (2008); Eur. Phys. J. C **56**, 333 (2008).
- [48] T. R. Slatyer, N. Padmanabhan, and D. P. Finkbeiner, Phys. Rev. D **80**, 043526 (2009).
- [49] S. Coutu *et al.*, in *Proc. 27th Int. Cosmic Ray Conference, Hamburg* (IUPAP, Hamburg, 2001), Vol. 5, p. 1687.